

The orbital periods of subdwarf B binaries produced by the first stable Roche overflow channel

Xuefei Chen^{1,2*} Zhanwen Han^{1,2} Jan Deca³ and Philipp Podsiadlowski⁴

¹ Yunnan Observatory, Chinese Academy of Sciences, Kunming, 650011, China

² Key Laboratory for the Structure and Evolution of Celestial Objects, Chinese Academy of Sciences, Kunming, 650011, China

³ Centrum voor Plasma-Astrofysica, Katholieke University Leuven, Celestijnenlaan 200B, B-3001 Leuven, Belgium

⁴ University of Oxford, Department of Astrophysics, Keble Road, Oxford OX1 3RH

13 June 2021

ABSTRACT

Long-orbital-period subdwarf B (sdB) stars with main-sequence companions are believed to be the product of stable Roche Lobe overflow (RLOF), a scenario challenged by recent observations. Here we represent the results of a systematic study of the orbital-period distribution of sdB binaries in this channel using detailed binary evolution calculations. We show that the observed orbital-period distribution of long-period sdB binaries can be well explained by this scenario. Furthermore, we find that, if the progenitors of the sdB stars have initial masses below the helium flash mass, the sdB binaries produced from stable RLOF follow a unique mass – orbital period relation for a given metallicity Z ; increasing the orbital period from ~ 400 to ~ 1100 d corresponds to increasing the mass of the sdB star from ~ 0.40 to $\sim 0.49 M_{\odot}$ for $Z = 0.02$. We suggest that the longest sdB binaries (with orbital period > 1100 d) could be the result of atmospheric RLOF. The mass – orbital period relation can be tested observationally if the mass of the sdB star can be determined precisely, e.g. from asteroseismology. Using this relation, we revise the orbital period distribution of sdB binaries produced by the first stable RLOF channel for the best fitting model of Han et al (2003), and show that the orbital period has a peak around 830 d.

Key words: binaries: close — sub-dwarfs — white dwarfs

1 INTRODUCTION

In the Hertzsprung-Russell diagram, subdwarf B stars (sdBs) are located between the main sequence (MS) and the white dwarf (WD) cooling track at the blueward extension of the horizontal branch. These objects play an important role in the study of stellar evolution theory, asteroseismology, as distance indicators and for Galactic structure and evolution (see the review of Heber 2009). They are also thought to be sources of far-ultraviolet radiation in early-type galaxies (Ferguson et al. 1991; Brown et al. 2000; Han et al 2007).

SdBs are generally considered to be helium-core-burning stars with extremely thin hydrogen envelopes ($< 0.02 M_{\odot}$) (Heber 1986; Saffer et al. 1994). Han et al. (2002, 2003) developed a detailed binary model for the formation of sdBs, which successfully explains field sdBs and possibly *extreme horizontal-branch* stars in globular clusters (Han 2008). They defined three types of formation channels to produce sdBs: the first and second stable Roche Lobe overflow (RLOF) channel for sdB binaries with long orbital pe-

riods, the first and second common envelope (CE) ejection channel for binary systems with short orbital periods, and the helium WD merger channel for single sdBs. Han et al. (2003) showed that the contribution of the second RLOF scenario is not significant. This means that most long-orbital period sdB binaries formed via stable RLOF channels must have MS companions. Such sdBs are hard to detect because of their bright companions and slow variability with time. The first stable RLOF channel therefore has remained untested due to the observational absence of long-period sdB binaries with known orbital periods.

Recently, Østensen & Van Winckel (2012) published a first sample of long-period sdB systems using data from the High Efficiency and Resolution Mercator Echelle Spectrograph mounted at the Mercator telescope in La Palma, Spain (Mercator sample hereinafter). Deca et al. (2012) reported a 760 d period for PG 1018-047. In addition, Barlow et al. (2012) determined precise orbital solutions for three systems by combining 6 years of Hobby-Eberly Telescope data with recent observations from the Mercator telescope. They present an up-to-date period histogram for all known hot subdwarf binaries, suggesting a long period peak to be

* E-mail: cxf@ynao.ac.cn

around 500 – 1000 d. All these observations seem to challenge the predictions of Han’s conventional model, which presented a period peak around 100 d and showed hardly any systems beyond 500 d.

This conflict results from a simplified treatment of the stable RLOF channel in the binary population synthesis study in Han et al. (2003) (hereinafter HPMM03), who were mainly interested in the CE channel, since only short-period sdB binaries had been found at the time. HPMM03 set the final masses to be the core masses of the giants at the onset of RLOF and obtained the final orbital periods by assuming that the lost mass takes away the angular momentum from the companion star. Such a treatment is obviously too simple and can result in significant discrepancies with observations; e.g. table 4 in Han et al. (2002) shows that sdBs are significantly heavier than the core mass of their giant at the onset of RLOF, and that systems can have orbital periods far beyond 500 d if the giant is less than $1.6 M_{\odot}$. This illustrates the necessity for improving the determination of the orbital period distribution for sdB binaries evolved through the first RLOF channel, using full binary evolution calculation rather than the simplified approach adopted in this earlier study.

In fact, there are two subchannels for the first stable RLOF channel. (i) If the primary has an initial zero-age main sequence mass (ZAMS) below the helium flash mass (about $2 M_{\odot}$ for Pop I), RLOF has to occur near the tip of the first giant branch (FGB), which leads to relatively long-period sdB+MS binaries (> 400 d as seen in Table 4 of Han 2002). (ii) If the ZAMS mass of the primary is larger than the helium flash mass and the system experiences stable RLOF in the Hertzsprung gap (HG) or on the FGB, this also leads to the formation of an sdB star, but with an orbital period likely less than 100 d as shown by Han et al. (2002), Chen & Han (2002, 2003). In this work we will mainly focus on the first subchannel, as it is the more important one and the only one that is relevant to explain the newly discovered systems.

In section 2, we introduce the stellar evolution code used and the basic inputs needed for the study. The evolutionary consequences, including the mass – orbital period relation are presented in section 3. In section 4 we discuss the sdB binaries with the longest orbital periods (> 1100 d). The orbital period distribution is presented in section 5, and our main conclusions are summarized in section 6.

2 BINARY EVOLUTION CALCULATIONS

We use the stellar evolution code originally developed by Eggleton (1971, 1972, 1973), updated with the latest input physics (Han et al. 1994; Pols et al. 1995, 1998). We set the mixing length to a local pressure scale height ratio $\alpha = 2.0$ ($\alpha = l/H_p$), the convective overshooting parameter, δ_{OV} , is set to 0.12 (Schröder et al. 1997), which roughly corresponds to an overshooting length of $0.25 H_p$. We study four metallicities, i.e. $Z = 0.02, 0.01, 0.004$ and 0.001 . The opacity tables for these metallicities were compiled by Chen & Tout (2007) from Iglesias & Rogers (1996) and Alexander & Ferguson (1994).

For each Z , the initial hydrogen mass fraction is obtained by $X = 0.76 - 3Z$ (Pols et al. 1998). The donor

stars can have four initial masses, i.e. $M_{1i} = 0.8, 1.00, 1.26$ or $1.6 M_{\odot}$, always lower than the helium flash mass for the respective Z value. The corresponding companion masses, M_{2i} , are 0.7, 0.9, 1.1 and $1.5 M_{\odot}$, respectively, chosen to be less than the donor star mass and at the same time ensuring stable RLOF, i.e. the mass ratio q (\equiv the donor/the accretor) is below the critical mass ratio q_c . The initial orbital period distribution is produced as follows: for orbital periods $P_i > 100$ d, we use intervals of 50 d, whereas for shorter periods a 20 d interval is chosen, in order to ensure that sdB stars can be produced with the corresponding assumptions. RLOF is included in the model via the following boundary condition:

$$\frac{dm}{dt} = C \cdot \text{Max}[0, (\frac{R}{R_L} - 1)^3], \quad (1)$$

where dm/dt is the mass-loss rate of the giant due to RLOF. The constant C is set to $500 M_{\odot} \text{yr}^{-1}$ so that RLOF can proceed steadily and the lobe-filling star overfills its Roche lobe as necessary but never overfills its lobe by much. Due to convergence problems, we artificially fix the maximum value of dm/dt at $0.5 \times 10^{-4} M_{\odot} \text{yr}^{-1}$ to make sure that most of the model runs evolve to the helium flash (or helium WD) successfully¹.

We define β as the fraction of mass lost by the donor via RLOF accreted onto the secondary. Three values of β (0, 0.5 and 1) have been studied². The remaining part, $1 - \beta$, is lost from the binary and takes away the specific angular momentum (marked with a parameter A) as pertains to the donor ($A = 1$), or to the companion ($A = 2$). A Reimers-type wind with an efficiency of $\eta = 1/4$ (Renzini 1981; Iben & Renzini 1983; Carraro et al. 1996) is included before the onset of RLOF. The wind is lost from the binary by taking away the specific angular momentum as pertains to the giant.

3 EVOLUTIONARY CONSEQUENCES

For each metallicity, the model produces three different outcomes: sdB+MS binaries, He WD binaries (where the helium flash does not occur) and red clump star binaries (RCS, where the helium flash occurs when the donor has an envelope mass larger than $0.0200 M_{\odot}$)³. Figure 1 summarizes the remnant mass (M_f) versus the orbital period (P) for all of these products. We use filled circles for sdB stars produced under the various assumptions, with red, green, blue, light blue and purple symbols respectively for $(\beta = 0, A = 2)$; $(\beta = 0.5, A = 2)$; $(\beta = 0, A = 1)$, $(\beta = 0.5, A = 1)$ and $(\beta = 1$ (independent on A for this case)). See also Table 1. Note that there is a clear $M_f - P$ correlation for sdB and He WD binaries for a given metallicity, while for the red clump

¹ The choice of this value has no influence on the final conclusions, in particular the sdB mass – period relation, which is independent of both the mass-loss rate and the angular momentum loss, as shown in this work.

² Since the donor is now a giant, RLOF is unlikely to be conservative. The value of $\beta = 1$ is included here for completeness of the calculations only.

³ The maximum hydrogen envelope mass of sdB stars is related to the core mass and metallicity and is around $0.02 M_{\odot}$ (Heber 2009).

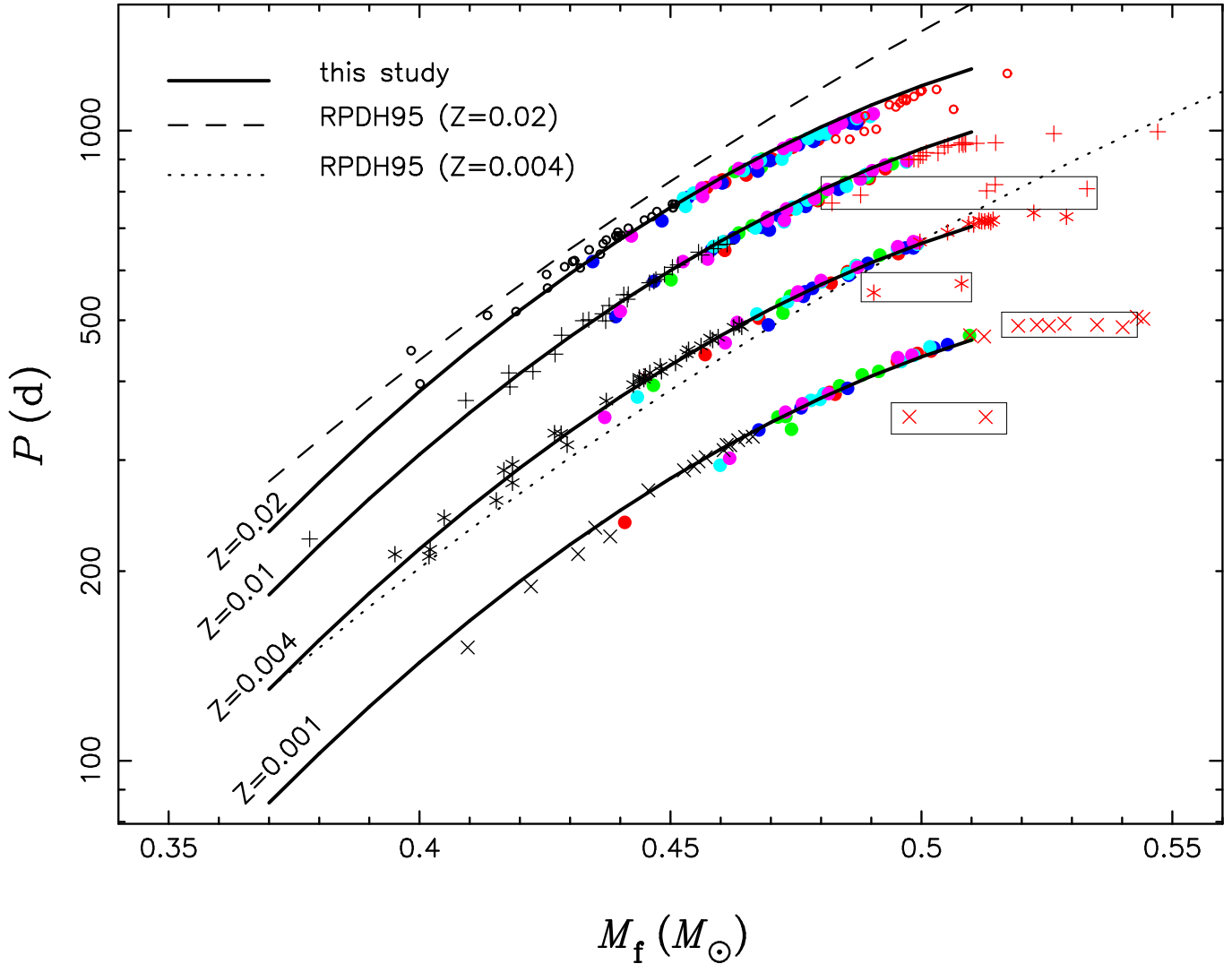


Figure 1. The remnant mass (M_f) – orbital period plane for binaries produced in this study. The filled circles are sdB+MS stars, where different colors represent those produced under different assumptions. Red, green, blue, light blue and purple filled circles represent $\beta = 0, A = 2$; $\beta = 0.5, A = 2$; $\beta = 0, A = 1$, $\beta = 0.5, A = 1$ and $\beta = 1$ (independent of A for this case), respectively (see also Table 1). From top to bottom, the metallicity is 0.02, 0.02, 0.004 and 0.001, respectively. Open circles, pluses, asterisks and crosses are for He WDs (low-mass end) and RCSs (high-mass end) at various metallicities, $Z = 0.02, 0.01, 0.004$ and 0.001 , respectively. Symbols enclosed in a rectangle are RCSs with similar orbital periods but different sdB masses. The dashed and dotted curves show the results from Rappaport et al. (1995)(RPDH95), i.e. Eq(6) of that paper with $R_0 = 5500$ and $3300 R_\odot$ for $Z = 0.02$ and 0.004 , respectively, while the solid curves are from the fitting formulae of this study.

binaries there is no clear trend, as one would expect (see sect. 3.1 for further discussion).

3.1 The $M_f - P$ relation

Giant donor stars generally have degenerate cores and follow the well-known $M_c - R$ (core mass – radius) relation (Refsdal & Weigert 1971; Webbink, Rappaport & Savonije 1983; Joss, Rappaport & Lewis, 1987). For a given core mass M_c , we can obtain the stellar radius R of the giant and hence its Roche lobe radius, R_L , which is $\approx R$. This directly constrains the orbital period and leads to a well-defined $M_c - P$ relation during stable RLOF. Roche lobe overflow stops when the donor star envelope collapses, i.e. when $M_f \simeq M_c$. This then defines a $M_f - P$ relation, which is independent of the an-

gular momentum loss during the mass-transfer phase. Since the stellar radius decreases with decreasing metallicity, the orbital period P will decrease with decreasing Z at a given M_f as shown in Figure 1.

The $M_f - P$ relation indicates that the remnant mass of the giant and the final orbital period after RLOF are coupled together. The way angular momentum is lost determines the remnant mass; e.g., rapid angular momentum loss leads to a shorter RLOF phase and a lower remnant mass for a given donor mass. This relation was first proposed by Rappaport et al. (1995)(RPDH95 hereinafter) and verified by many authors i.e. Tauris & Savonije (1999), Nelson, Dubeau & MacCannell (2004), De Vito & Benvenuto (2010, 2012), although there are some differences in the detailed proposed forms of this relation. These differences probably

arise from differences between the stellar evolution models (and codes) used.

RPDH95 obtained the $M_{\text{wd}} - P$ relation (where M_{wd} is the mass of the WD remnants after stable RLOF) in wide binary radio pulsars, according to the $M_c - R$ relation of single giants. For comparison, we show the results of RPDH95 in Fig. 1. Our result differs slightly from that of RPDH95 because of three factors: (i) We used updated opacities, which directly affect the stellar radius. Also, the Pop I models used in RPDH95 have $2 < \alpha < 3$ and various He abundances, both influencing the stellar radius and hence the final orbital period. (ii) The giant expands when losing mass, resulting in a small amount of divergence of the $M_c - R$ relation derived from single stars. (iii) The remnant mass of the giant is not exactly equal to its core mass at the termination of RLOF. In general, a more massive core has larger surface gravity, and the envelope starts to collapse when it is still quite thick. Therefore the orbital period increases more slowly (with M_f increasing) than expected from the $M_c - R$ relation for both Pop I and Pop II stars.

For RCSs, the envelope is too thick ($> 0.02 M_\odot$) at the He flash for the assumption of $M_f \approx M_c$ to be valid. In this case, the orbital period is in fact determined by the core mass of the RCS, as is also partly reflected in Fig. 1. For example, there are five pluses with orbital periods around 800 d (enclosed in a rectangle), but with masses in a wide range ($0.48 - 0.53 M_\odot$). The ZAMS masses of the donors in the five systems are $1.6 M_\odot$ and their core masses are around $0.45 M_\odot$. There are several similar cases shown in this figure, i.e. two lower asterisks, two lower crosses, crosses with mass larger than $0.51 M_\odot$ (enclosed in the rectangles of Fig. 1) etc. The systems in a particular rectangle have similar orbital periods since the donors have similar core masses at the He flash.

3.2 The fitting formulae

For convenience, we have fitted the $M_f - P$ relation with a polynomial formula for $Z = 0.004^4$:

$$\log P = c_1 + c_2 M_f + c_3 M_f^2, \quad (2)$$

with P in days and M_f in solar mass. The coefficients are $c_1 = -3.5605$, $c_2 = 22.6555$ and $c_3 = -19.7851$, with a maximum error of 1.1 percent in P . The orbital period for other metallicities at a given M_f can be obtained by a simple vertical shift of Eq(2), i.e. changing the value of the constant c_1 . For $Z = 0.02$, 0.01 and 0.001 , we find $c_1 = -3.3105$, -3.4105 and -3.7505 , respectively, with the maximum fitting error being 2.9, 1.1 and 1.4 percent in P , respectively⁵. This means that for different metallicities, the orbital period increases at a similar rate (with M_f), which is to be expected since all the binaries have evolved by stable RLOF. The fitting formulae are plotted in Fig. 1 as solid curves.

⁴ We choose $Z = 0.004$ because the sample distribution in the mass range of $0.39 - 0.51 M_\odot$ are more uniform for this metallicity than others.

⁵ The overall best fit for $Z = 0.02$ is $c_1 = -1.8203$, $c_2 = 16.5762$, and $c_3 = -13.6420$ in Eq(2), with a maximum error of 1.2 percent in P .

3.3 PG 1018-047

PG 1018-047 is a long-orbital-period sdB binary whose MS companion and orbital parameters have been studied in detail, allowing direct constraints of the stable RLOF channel. It has a mid-K (K3-K5) MS companion with an orbital period of 759 ± 5.8 d and a mass ratio (MS/sdB) of 1.6 ± 0.2 . If PG 1018-047 has indeed a circular orbit, it is a good candidate to have formed via first stable Roche lobe overflow (Deca et al. 2012). However, for this system to have evolved within a Hubble time with close-to-conservative mass transfer, the present K star must have been no heavier than $\sim 0.3 - 0.4 M_\odot$, leading to a contradiction with the initial mass ratio of the binary. We refer to Deca et al. (2012) for an elaborate discussion.

Previous studies have shown that non-conservative RLOF (Han et al. 2002; Chen & Han 2008) or a small mass ratio (the ratio of donor to accretor mass) or both most likely lead to stable RLOF, indicating that PG 1018-047 is likely the product of non-conservative RLOF, with $Z = 0.01 - 0.02$ (from Fig. 1). This metallicity indicates PG 1018-047 possible to be a thin disk star. On the other hand, its location, R.A.(J2000): 10h 21m 10.50s, DEC(J2000): $-04^\circ 56' 19.3''$ (Deca 2010) seems to suggest a halo star. A high-resolution spectroscopic study of PG 1018-047, including metallicity constraints, is well under way and should help to address this issue in more detail in the future.

4 THE LONGEST PERIOD (> 1100 D) SDB BINARIES

Figure 1 shows that sdB binaries produced by the first stable Roche lobe overflow channel have a narrow mass range and hence a limited range of possible orbital periods. For $Z = 0.02$, the orbital period changes from ~ 600 to 1100 d as the sdB mass increases from ~ 0.43 to $\sim 0.49 M_\odot$ ⁶. The longest system in our calculations has $P = 1063$ d with a mass of $0.4904 M_\odot$ for this metallicity (see Table 1). According to the $M_f - P$ relation, the upper limit of the orbital period is determined by the maximum sdB mass, which can be estimated by the sum of the maximum core mass of the giant on the FGB ($M_c^{\text{tip}} = 0.4746 M_\odot$, see Table 1 in Han et al. 2002) and the maximum envelope mass allowed for sdB stars ($0.02 M_\odot$). The maximum sdB mass is then $0.4946 M_\odot$, which corresponds to an orbital period of 1135 d.

There are three sdB+MS binaries with orbital periods longer than 1100 d, i.e. BD+29°3070, BD-7°5977 and PG1317+123. Their orbital periods are 1160, 1194 and 1179 d, respectively (Østensen & Van Winckel 2012, Barlow et al. 2012). If we consider observational errors for the three objects (67, 79 and 12 d, respectively) and the uncertainties on stellar radius in the model calculations, the three systems are consistent with the $M_f - P$ relation.

In our binary evolution, the RLOF switches on (off) sharply when the radius of the donor is larger (smaller) than its Roche lobe radius. However this assumption does

⁶ The lower limit of orbital period can be as low as ~ 400 d when the donor's ZAMS mass is $1.9 M_\odot$, see Table 4 of Han et al. (2002).

Table 1. The sdB mass (M_{sdb}) and orbital period (P) of sdB+MS binaries in our studies. The first two columns show the ZAMS masses of the donors (M_{1i}) and the initial orbital periods (P_i), respectively. The companion masses are 0.7, 0.9, 1.1 and $1.5 M_{\odot}$ for $M_{1i} = 0.79, 1.00, 1.26$ and $1.6 M_{\odot}$, respectively. The initial orbital periods are different for different cases to ensure that sdB stars are produced with the corresponding assumptions. The interval of P_i is ~ 50 d when $P_i > 100$ d and 20 d when $P_i < 100$ d. β is the fraction of the mass lost from the donor via RLOF accreted onto the secondary, and A is a label for the angular momentum loss; it is 1, if the mass lost from the system takes away the same specific angular momentum as the donor, and 2, if it the specific angular momentum of the accretor. The results are independent of A for the case $\beta = 1.0$ (conservative mass transfer). The masses and orbital period are in units of solar masses and days, respectively.

$Z = 0.02$				$Z = 0.01$				$Z = 0.004$				$Z = 0.001$			
M_{1i}	P_i	M_{sdb}	P	M_{1i}	P_i	M_{sdb}	P	M_{1i}	P_i	M_{sdb}	P	M_{1i}	P_i	M_{sdb}	P
$\beta = 0$															
$A=2$															
0.79	400.0	0.4608	829.2	0.79	350.0	0.4683	704.3	0.79	250.0	0.4676	504.0	0.79	200.0	0.4828	381.6
0.79	450.0	0.4703	900.6	0.79	400.0	0.4794	774.1	0.79	300.0	0.4820	572.6	0.79	250.0	0.5019	446.8
0.79	500.0	0.4794	968.5	0.79	450.0	0.4896	839.3	0.79	350.0	0.4954	637.9	1.00	150.0	0.4952	430.0
1.00	250.0	0.4603	835.1	1.00	200.0	0.4608	665.9	1.00	200.0	0.4853	597.3	1.26	80.0	0.4817	384.2
1.00	300.0	0.4743	940.9	1.00	250.0	0.4775	772.0	1.60	40.0	0.4569	441.1	1.26	100.0	0.4992	442.9
1.00	351.0	0.4876	1041.0	1.00	300.0	0.4928	870.1					1.58	20.0	0.4409	238.9
1.26	150.0	0.4572	812.0	1.26	150.0	0.4736	748.3								
1.26	200.0	0.4786	975.2	1.60	60.0	0.4608	645.7								
1.60	80.0	0.4651	850.1												
$\beta = 0.5$															
$A=2$															
0.79	450.0	0.4601	831.7	0.79	400.0	0.4692	715.6	0.79	300.0	0.4722	530.2	0.79	200.0	0.4730	351.9
0.79	500.0	0.4689	897.0	0.79	450.0	0.4792	779.4	0.79	350.0	0.4852	593.1	0.79	250.0	0.4915	414.9
1.00	300.0	0.4628	860.9	0.79	500.0	0.4893	843.3	0.79	400.0	0.4978	654.5	0.79	300.0	0.5096	473.0
1.00	351.0	0.4751	955.2	1.00	250.0	0.4663	706.0	1.00	200.0	0.4739	546.0	1.00	150.0	0.4837	393.6
1.00	400.0	0.4868	1044.0	1.00	300.0	0.4804	797.6	1.00	250.0	0.4917	634.3	1.26	80.0	0.4714	351.1
1.26	200.0	0.4682	900.7	1.00	350.0	0.4942	885.5	1.26	150.0	0.4870	610.9	1.26	100.0	0.4882	409.6
1.26	250.0	0.4853	1033.0	1.26	150.0	0.4636	688.0	1.60	40.0	0.4466	394.4	1.58	40.0	0.4741	335.8
1.60	80.0	0.4529	761.0	1.26	201.0	0.4849	827.5	1.60	60.0	0.4724	513.6				
1.60	100.0	0.4681	875.7	1.60	60.0	0.4501	579.9								
				1.60	80.0	0.4691	699.5								
$\beta = 0$															
$A=1$															
0.79	500.0	0.4603	825.9	0.79	450.0	0.4681	702.3	0.79	350.0	0.4765	545.7	0.79	250.0	0.4853	389.9
0.79	551.0	0.4698	896.3	0.79	500.0	0.4769	757.9	0.79	400.0	0.4855	589.2	0.79	300.0	0.5052	457.4
0.79	600.0	0.4785	961.3	1.00	350.0	0.4626	675.9	0.79	450.0	0.4984	651.3	1.00	200.0	0.4760	363.2
0.79	650.0	0.4871	1026.0	1.00	400.0	0.4716	732.5	1.00	300.0	0.4783	561.9	1.00	250.0	0.5025	452.1
1.00	400.0	0.4535	783.5	1.00	450.0	0.4879	838.1	1.00	350.0	0.4893	615.6	1.26	150.0	0.4676	334.9
1.00	450.0	0.4648	867.5	1.26	300.0	0.4582	647.3	1.26	250.0	0.4768	554.7				
1.00	500.0	0.4755	949.4	1.26	350.0	0.4765	764.7	1.26	301.0	0.4968	651.2				
1.00	550.0	0.4860	1028.0	1.26	400.0	0.4846	816.2	1.60	200.0	0.4695	491.6				
1.26	400.0	0.4689	897.8	1.26	450.0	0.4835	806.9								
1.26	451.0	0.4817	996.2	1.60	200.0	0.4391	506.7								
1.26	500.0	0.4807	986.7	1.60	250.0	0.4561	611.9								
1.60	250.0	0.4345	619.7	1.60	300.0	0.4697	695.2								
1.60	300.0	0.4483	719.0												
$\beta = 0.5$															
$A=1$															
1.60	350.0	0.4674	862.4	0.79	450.0	0.4669	700.7	0.79	350.0	0.4733	535.0	0.79	250.0	0.4798	374.5
0.79	500.0	0.4553	795.6	0.79	500.0	0.4750	751.0	0.79	400.0	0.4854	593.4	0.79	300.0	0.4960	429.9
0.79	551.0	0.4645	863.7	0.79	550.0	0.4851	815.9	0.79	450.0	0.4992	660.4	1.00	200.0	0.4806	382.3
0.79	600.0	0.4730	927.6	0.79	600.0	0.4970	891.4	1.00	300.0	0.4801	575.6	1.00	250.0	0.5017	453.8
0.79	650.0	0.4812	989.1	1.00	350.0	0.4605	666.3	1.00	350.0	0.4952	650.2	1.26	150.0	0.4780	373.1
0.79	700.0	0.4898	1053.0	1.00	400.0	0.4773	775.9	1.26	200.0	0.4672	511.8	1.26	200.0	0.4985	440.0
1.00	400.0	0.4526	781.0	1.00	450.0	0.4889	851.4	1.26	251.0	0.4870	609.8	1.58	80.0	0.4599	294.5
1.00	450.0	0.4673	894.3	1.26	250.0	0.4586	655.0	1.60	100.0	0.4434	377.7				
1.00	500.0	0.4774	971.6	1.26	300.0	0.4743	755.8								
1.00	550.0	0.4871	1045.0	1.26	350.0	0.4888	850.8								
1.26	300.0	0.4546	796.0	1.60	200.0	0.4726	716.2								
1.26	350.0	0.4679	897.1												
1.26	400.0	0.4796	987.6												
1.60	200.0	0.4530	758.1												
1.60	251.0	0.4722	900.7												
$\beta = 1.0$															
0.79	500.0	0.4589	827.1	0.79	450.0	0.4693	720.0	0.79	350.0	0.4752	547.9	0.79	250.0	0.4815	382.6
0.79	551.0	0.4672	889.1	0.79	500.0	0.4787	780.0	0.79	400.0	0.4873	606.7	0.79	300.0	0.4981	440.3
0.79	600.0	0.4749	947.7	0.79	550.0	0.4878	838.7	0.79	450.0	0.4991	663.8	1.00	150.0	0.4729	357.5
0.79	650.0	0.4827	1006.0	0.79	600.0	0.4971	896.1	1.00	200.0	0.4633	495.9	1.00	200.0	0.4953	436.3
0.79	700.0	0.4904	1063.0	1.00	301.0	0.4693	728.1	1.00	250.0	0.4800	578.4	1.26	100.0	0.4763	368.7
1.00	351.0	0.4636	870.2	1.00	350.0	0.4813	806.4	1.00	300.0	0.4953	654.2	1.58	40.0	0.4618	302.0
1.00	400.0	0.4740	949.4	1.00	400.0	0.4928	881.4	1.26	150.0	0.4754	554.4				
1.00	451.0	0.4841	1028.0	1.26	150.0	0.4525	619.6	1.26	200.0	0.4984	666.5				
1.26	200.0	0.4563	810.8	1.26	201.0	0.4731	751.2	1.60	40.0	0.4369	350.8				
1.26	250.0	0.4725	936.9	1.26	250.0	0.4902	863.8	1.60	60.0	0.4609	460.4				
1.26	300.0	0.4873	1051.0	1.60	60.0	0.4400	516.7								
1.60	80.0	0.4422	680.5	1.60	80.0	0.4574	625.3								
1.60	100.0	0.4564	786.1	1.60	100.0	0.4727	720.8								

not take into account the possibility of material (atmosphere) outside the photospheric stellar radius. This means that, when the stellar radius approaches the Roche Lobe radius, some atmospheric material will already overflow the Roche lobe and be transferred to the companion (Ritter 1988, Pastetter & Ritter, 1989; Podsiadlowski et al. 2002, Chen et al. 2010). This is referred to as atmospheric RLOF. In this case, the Roche Lobe is larger than the stellar radius during mass transfer, resulting in a larger separation and thus a longer orbital period. If the underfilling fac-

tor is 10 percent as suggested by S-type symbiotics with ellipsoidal variability (Rutkowski, Mikolajewska & Whitelock 2007; Otulakowska-Hypka, Mikolajewska & Whitelock 2013), the Roche lobe radius R_L , and hence the separation a , are 1.1 times larger than before. The orbital period P will then be 1.17 times longer because $P \propto a^{3/2}$. Some sdB binaries with orbital periods of 940 – 1025 d will then be shifted into the 1100 – 1200 d range, significantly increasing

the number of sdB+MS binaries with orbital period longer than 1100 d in the model⁷.

Furthermore, there may be other channels, e.g. a tidally enhanced stellar wind channel or an envelope ejection channel at the tip of the FGB (Han et al. 2010) that can also lead to sdB+MS binaries with very long orbital periods.

5 THE ORBITAL PERIOD DISTRIBUTION

In order to investigate the orbital period distribution of sdB binaries from the stable RLOF, we have performed a Monte Carlo simulation similar to those of HPMM03 but with the latest version of the binary population synthesis code. The simulation is for a Population I population and the required parameters in the Monte Carlo simulation are the same as those in HPMM03 i.e. the star formation rate is taken to be constant over the last 15 Gyr, the initial mass function of the primary are from a simple approximation of Miller & Scalo (1979), the initial mass-ratio (q , the ratio of the secondary to primary mass) distribution is also set to be constant ($n(q) = 1, 0 < q \leq 1$), all stars are assumed to be members of binaries and the distribution of separations (a) is constant in $\log a$ for wide binaries and falls off smoothly at close separations. The critical mass ratio for dynamically stable mass transfer between giants and their companions, q_{crit} , the common-envelope ejection efficiency, α_{CE} , and the thermal contribution to the CE ejection, α_{th} , are set to be 1.5, 0.75 and 0.75, respectively, the same as that of the best fitting model of HPMM03 (set 2 in that paper).

As described in section 1, there are two subchannels, one for progenitors with ZAMS mass less than $2 M_{\odot}$, one for progenitors with ZAMS mass greater than $2 M_{\odot}$, that lead to the formation of sdB long-period binaries. For the subchannel of progenitors with ZAMS mass less than $2 M_{\odot}$, the sdB binaries follow the unique mass – orbital period relation. The sdB mass produced from stable RLOF is determined by the details of the mass transfer process. For simplicity, we assume that the masses of the sdB stars produced in this way are uniformly distributed between $M_{\text{sdB}}^{\text{min}}$ and $M_{\text{sdB}}^{\text{max}}$ if the ZAMS mass of the donor is less than $2 M_{\odot}$ (the helium flash mass for Population I), where $M_{\text{sdB}}^{\text{min}} = 0.4570, 0.4552, 0.4550, 0.4425$ and $0.4064 M_{\odot}$, $M_{\text{sdB}}^{\text{max}} = M_{\text{c}}^{\text{tip}} + 0.02 = 0.4946, 0.4927, 0.4923, 0.4801$ and $0.4287 M_{\odot}$, for the donor’s mass of 0.8, 1.0, 1.26, 1.6 and 1.9 M_{\odot} , respectively (see Tables 1 and 4 in Han et al. 2002). For other donor masses less than $2 M_{\odot}$, $M_{\text{sdB}}^{\text{min}}$ and $M_{\text{sdB}}^{\text{max}}$ are linearly interpolated from these five stars. The orbital period is then obtained from the fitting formulae in sect. 3.2.

For the subchannel of progenitors with ZAMS mass greater than $2 M_{\odot}$, the sdB mass and orbital period do not follow the sdB mass – orbital period relation, but the orbital period depends on both the sdB mass and the amount of angular momentum loss, which are obtained in a way similar to that of HPMM03. The sdB mass is taken from the detailed binary evolution models of Han et al. (2000) when

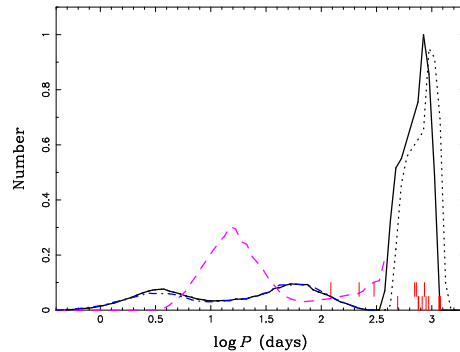


Figure 2. The distribution of orbital periods of sdB stars from the first stable RLOF. Different curves are for different assumptions for systems with donor ZAMS masses larger than $2 M_{\odot}$; solid: the final mass of the donor is obtained from Han et al. (2000) and the mass lost from the system takes away the specific angular momentum as pertains to the system [the standard set]; dash-dotted: the final mass of the donor is obtained from the non-conservative binary calculations of Chen & Han (2002), in comparison to the standard set; dashed: the mass lost takes away the specific angular momentum as pertains to the donor in comparison to the standard set (the dashed and dash-dotted curves are plotted only for $\log P(\text{d}) < 2.6$ for clarity). The dotted curve is for atmospheric-RLOF i.e. the orbital periods of sdB stars from the He flash models are multiplied by 1.17 (see sect. 4 for details). Short ticks along and above the X-axis indicate the positions of sdB+MS stars in the observational sample for solved and unsolved long-orbital sdB stars, respectively (Østensen & Van Winckel 2012, Barlow et al. 2012, Deca et al. 2012).

RLOF begins in the HG or set to be the core mass of the donor at the onset of RLOF when RLOF starts on the FGB (since there no detailed study of this channel yet, using full binary evolution calculations), and 50 percent of the mass lost from the donor is lost from the system, taking away the same specific angular momentum as pertains to the system. The orbital periods of sdB stars in this case are very sensitive to the assumptions about angular momentum loss, which will be discussed at the end of this section.

Fig. 2 shows the orbital period distribution of sdB binaries from the first stable RLOF channel. The distribution (the solid curve) has two parts, separated by a well-defined gap. The left-hand part contains systems where the ZAMS mass of the donor is larger than $2 M_{\odot}$ and the right-hand part are systems with ZAMS donor masses less than $2 M_{\odot}$. The gap is caused by the sharp drop of the radius at the tip of FGB from stars with ZAMS masses somewhat smaller than $2 M_{\odot}$ (the helium flash mass for Pop I) relative to stars with ZAMS masses somewhat greater than $2 M_{\odot}$ (see Han et al. 2002). The left-hand part has two peaks: the first peak (~ 4 d) is from systems undergoing RLOF during the HG while the second peak (~ 63 d) comes from systems undergoing RLOF on the FGB. The second peak was originally buried in the main peak of the dashed curve of Fig. 10 in HPMM03, and appears when sdB stars from systems with ZAMS donor mass smaller than $2 M_{\odot}$ have been shifted to longer orbital periods. The donors of binaries that produce the second peak have non-degenerate cores on the FGB, and their behaviour is somewhat different from those with degenerate cores, e.g. there is no sudden collapse of the envelope at the end of RLOF. Thus, sdB stars from these systems

⁷ The effect of atmospheric RLOF discussed here is just an informed estimate, and the corresponding period distribution shown in Fig. 2 is re-scaled from that obtained without atmospheric-RLOF. Detailed calculations with atmospheric-RLOF implemented may reveal some differences.

will not exactly follow the mass-orbital period relation obtained from the donors with degenerate cores. Detailed binary evolution calculations are necessary to improve modeling of such systems, which we leave for a future study.

The right-most peak in the period distribution lies between $\sim 400 - 1100$ d with a peak around 830 d. Most observed long-orbital period sdB stars fall into this range, i.e. can be well explained by this channel. Taking into account the possibility of atmospheric RLOF may extend this range to orbital periods as long as ~ 1600 d (the dotted curve), and could easily explain the longest period sdB binaries (> 1100 d) known to-date. There are three sdB stars with orbital periods less than 400 d but longer than 100 d. They are unsolved systems and further observations are necessary to confirm their orbital periods. They may not come from the first stable RLOF for Pop I stars if their orbital periods are in this range. The first CE ejection channel is a possible channel can produce sdB+MS binaries with orbital periods between 100 and 400 d. HPMM03 pointed out that the upper limit of the orbital period distribution from the first CE channel could be as long as 400 d in the extreme case of $\alpha_{\text{CE}} = \alpha_{\text{th}} = 1$.

As shown in sect. 3, the orbital period of sdB stars from the first stable RLOF with ZAMS donor mass smaller than $2 M_{\odot}$ is only dependent on the sdB mass. The whole right-most peak of the period distribution in Fig. 2 then cannot be affected by the assumed angular momentum loss. But the left-hand part of the distribution is significantly influenced by this assumption. If we assume that the mass lost takes away the same specific angular momentum as pertains to the donor (significantly smaller than that of system) rather than to the system, the orbital periods of sdBs become longer, and the first orbital period peak moves to ~ 16 d while the second peak now overlaps with the right-hand part (the dashed curve). In general, as one would expect, a smaller amount of angular momentum loss leads to longer orbital periods. So, the observed orbital period distribution for sdB stars with masses significantly diverging from $\sim 0.48 M_{\odot}$ (sdB stars with mass around $0.48 M_{\odot}$ are likely from the first CE channel) can be used to constrain the angular momentum loss during RLOF in the HG directly. Since the donors do not suffer a sudden collapse of the envelope at the end of RLOF if their ZAMS masses are larger than $2 M_{\odot}$, the orbital period distribution of sdB star mass from these systems is not sensitive to the sdB mass. We see from Fig. 2 that, if we adopt the final masses of the donors obtained from non-conservative calculations (e.g. Chen & Han, 2002), the orbital period distribution (the dash-dotted curve) is similar to that obtained from conservative calculations.

6 SUMMARY

In this paper we have investigated the orbital periods of sdB stars produced from the first stable RLOF with ZAMS donor star masses somewhat lower than the helium flash mass. Using detailed binary stellar evolution calculations, we have determined a unique mass – orbital period relation for sdB stars and WD binaries produced in this way for various metallicities. This relation is a direct consequence of the core mass – radius relation of giant stars and the sudden collapse of the giants at the end of RLOF. Binaries with red

clump stars (RCSs) do not follow this relation because their envelopes are too thick at the He flash and the donors have not yet suffered a sudden collapse of their envelopes. The final orbital period of RCSs is then determined by the core mass of the donor at the He flash, not the mass of the RCSs. The mass – orbital period relation can be verified from observations if the sdB mass could be precisely determined, e.g. from asteroseismology.

Implementing this mass – orbital period relation into binary population synthesis code, we re-evaluated the distribution of orbital periods of sdB stars from the first stable RLOF for a Population I distribution. There is a wide orbital period range i.e. from several days to ~ 1100 d for sdB stars produced from the first stable RLOF. If the ZAMS mass of the donors are less than $2 M_{\odot}$, the orbital period increases from ~ 400 to ~ 1100 d as the sdB mass increases from ~ 0.40 to $\sim 0.49 M_{\odot}$. The period peak is around 830 d, corresponding to a sdB mass of $\sim 0.46 M_{\odot}$. Most observed long-orbital-period sdB binaries are located in this range and are therefore well explained by this formation channel. The longest sdB binaries (with orbital period > 1100 d) are likely a consequence of atmospheric RLOF, while the sdB stars with orbital periods in the range of $100 - 400$ d may come from the first CE ejection channel.

ACKNOWLEDGMENTS

This work is partly supported by the NSFC (Nos. 10973036, 11173055, 11033008 and 11003003), the CAS (No. KJJCX2-YW-T24 and the Talent Project of Western Light)and the Talent Project of Young Researchers of Yunnan province (2012HB037).

REFERENCES

- Alexander D.R., Ferguson J.W., 1994, ApJ, 437, 879
- Barlow et al., 2012, ApJ, 758, 58
- Brown T. M., Bowers C. W., Kimble R. A., Sweigant A. V., Ferguson H. C., 2000, ApJ, 532, 308
- Carraro G., Girardi L., Bressan A., Chiosi C., 1996, A&A, 305, 849
- Chen X., Han Z., 2002, MNRAS, 335, 948
- Chen X., Han Z., 2003, MNRAS, 341, 662
- Chen X., Han Z., 2008, MNRAS, 387, 1416
- Chen X., Tout C. A., 2007, ChJAA, 7(No.2), 245
- Chen X., Podsiadlowski Ph., Mikolajewska J., Han Z., 2010, in Kolagera V. and van der Sluys M., eds, AIP Conf. Proc. 314, International Conference on Binaries, p.59
- Deca J., 2010, PG1018-047: The longest period subdwarf B binary (Unpublished master's thesis), Katholieke Universiteit Leuven, Leuven, Belgium
- Deca J. et al., 2012, MNRAS, 421, 2798
- De Vito M. A., Benvenuto O. G., 2010, MNRAS, 401, 2552
- De Vito M. A., Benvenuto O. G., 2012, MNRAS, 421, 2206
- Eggleton P. P., 1971, MNRAS, 151, 351
- Eggleton P. P., 1972, MNRAS, 156, 361
- Eggleton P. P., 1973, MNRAS, 163, 279
- Ferguson H. C. et al., 1991, 382, L69
- Han Z., 2008, A&A, 484, L31
- Han Z., Podsiadlowski Ph., Eggleton P. P., 1994, MNRAS, 270, 121
- Han Z., Podsiadlowski Ph., Lynas-Gray A. E., 2007, MNRAS, 380, 1098

- Han Z., Podsiadlowski Ph., Maxted P. F. L., Marsh T. R., Ivanova N., 2002, MNRAS, 336, 449
- Han Z., Podsiadlowski Ph., Maxted P. F. L., Marsh T. R., 2003, MNRAS, 341, 669 (HPMM03)
- Han Z., Tout C. A., Eggleton P. P., 2000, MNRAS, 319, 215
- Han Z., Chen X., Lei Z., 2010, AIPC, 1314, 85
- Heber U., 1986, A&A, 155, 33
- Heber U., 2009, ARA&A, 47, 211
- Iben I. Jr, Renzini A., 1983, ARA&A, 21, 271
- Iglesias C.A., Rogers F.G., 1996, ApJ, 464, 943
- Joss P. C., Rappaport S., Lewis W., 1987, ApJ, 319, 180
- Miller G. E., Scalo J. M., 1979, ApJS, 41, 513
- Nelson L. A., Dubeau E., MacCannell K. A., 2004, ApJ, 616, 1124
- Østensen R., Van Winckel H., 2012, in David Kilkeny, C. Simon Jeffery, and Chris Koen eds, ASP Conf. Ser. Vol.452, Fifth Meeting on Hot Subdwarf Stars and Related Objects, p.163
- Otulakowska-Hypka M., Mikolajewska J., Whitelock P.A., 2013, P. A. Woudt and V. A. R. M. Ribeiro, eds, STELLA NOVAE: FUTURE AND PAST DECADES, ASP Conference Series, in press.
- Pastetter L., Ritter H., 1989, A&A, 214, 186
- Podsiadlowski Ph., Rappaport S., Pfahl E. D., 2002, ApJ, 565, 1107
- Pols O. R., Schröder K. P., Hurley J. R., Tout C. A., Eggleton P. P., 1998, MNRAS, 298, 525
- Pols O. R., Tout C. A., Eggleton P. P., Han Z., 1995, MNRAS, 274, 964
- Rappaport S., Podsiadlowski Ph., Joss P. C., Di Stefano R., Han Z., 1995, MNRAS, 273, 731 (RPDH95)
- Refsdal S., Weigert A., 1971, A&A, 13, 367
- Renzini A., 1981, in Chiosi C., Stalio R., eds, Effects of Mass Loss on Stellar Evolution. Reidel, Dordrecht, p. 319
- Ritter H., 1988, A&A, 202, 93
- Rutkowski A., Mikolajewska J., Whitelock P.A., 2007, Baltic Astr. 16, p. 49
- Saffer R. A., Bergeron P., Koester D., Liebert J., 1994, ApJ, 432, 351
- Schröder K. P., Pols O. R., Eggleton P. P., 1997, MNRAS, 285, 696
- Tauris T. M., Savonije G. J., 1999, A&A, 350, 928
- Webbink R. F., Rappaport S., Savonije G. J., 1983, ApJ, 270, 678